Overexpression of a newly identified D-amino acid transaminase in *Mycobacterium smegmatis* complements glutamate racemase deletion

Roman Mortuza[1,2], Htin Lin Aung[2], George Taiaroa[2], Helen K. Opel-Reading[1], Torsten Kleffmann[1], Gregory M. Cook[2], Kurt L. Krause[1*]

[1] Department of Biochemistry, University of Otago, New Zealand

[2] Department of Microbiology and Immunology, University of Otago, New Zealand

[*]Corresponding Author: Kurt L. Krause, Dept. of Biochemistry, University of Otago, 710 Cumberland St., Dunedin 9016, New Zealand; Phone: +64 (0)21-074-4303, e-mail: kurt.krause@otago.ac.nz

Running Title: D-amino acid transaminase (D-AAT) from *Mycobacterium smegmatis*

Keywords: glutamate racemase, D-amino acid transaminase, alanine racemase, mycobacteria, drug design, tuberculosis, promoter, suppressor mutation, revertant phenotype, enzyme assay

Summary:

Glutamate racemase (MurI) has been proposed as a target for anti-tuberculosis drug development based on the inability of Δ*murI* mutants of *Mycobacterium smegmatis* to grow in the absence of D-glutamate. In this communication, we identify Δ*murI* suppressor mutants that are detected during prolonged incubation. Whole genome sequencing of these Δ*murI* suppressor mutants identified the presence of a SNP, located in the promoter region of MSMEG_5795. RT-qPCR and transcriptional fusion analyses revealed that the Δ*murI* suppressor mutant overexpressed MSMEG_5795 14-fold compared to the isogenic wild-type. MSMEG_5795, which is annotated as 4-amino-4-deoxychorismate lyase (ADCL) but which also has homology to D-amino acid transaminase (D-AAT), was expressed, purified and found to have D-AAT activity and to be capable of producing D-glutamate from D-alanine. Consistent with its D-amino acid transaminase function, overexpressed MSMEG_5795 is able to complement both Δ*murI* deletion mutants and alanine racemase (Δ*alr*) deletion mutants, thus confirming a multifunctional role for this enzyme in *M. smegmatis*.

Introduction

Mycobacterium tuberculosis, the etiologic agent of tuberculosis (TB), latently infects one third of the world's population, and in 2015 claimed 1.8 million lives according to WHO estimates (WHO, 2015). TB requires prolonged treatment, and non-adherence often results in the appearance of drug-resistance. Resistance to multiple drugs in TB is an ongoing threat to global health (WHO, 2017). Of the 10.4 million TB cases reported by the World Health Organization in 2015, 480,000 people were infected with either multi-drug resistant (MDR-TB) or extremely drug resistant (XDR-TB) strains (WHO, 2017). The treatments for drug resistant TB are often inefficacious as well as toxic, and the mortality rates of MDR-TB and XDR-TB have been reported as 63% and 88% respectively (Dheda *et al.*, 2014, WHO, 2017, Gandhi *et al.*, 2012). Therefore, finding new drugs to target *M. tuberculosis* will be necessary to control this globally important infectious disease.

Glutamate racemase (MurI) has been proposed recently as a potential new target for inhibition by anti-tuberculosis therapies (Li *et al.*, 2014, Morayya *et al.*, 2015, Poen *et al.*, 2016, Prosser *et al.*, 2016). MurI is an essential enzyme in most bacteria and it is needed to provide D-glutamate for completion of the peptidoglycan layer of the bacterial cell wall (Doublet *et al.*, 1993, Geng *et al.*, 2008). The *murI* gene has been reported as essential in *E. coli* (Doublet *et al.*, 1993), *Bacillus anthracis* (Oh *et al.*, 2015), *B. subtilis* (Kimura *et al.*, 2004), *Helicobacter pylori* (Lundqvist *et al.*, 2007) and *Streptococcus pneumoniae* (de Dios *et al.*, 2002), among others. Recent work has confirmed its essentiality in both *M. smegmatis* (Li *et al.*, 2014) and *M.*

tuberculosis (Morayya *et al.*, 2015, Griffin *et al.*, 2011), contradicting earlier studies (Sassetti *et al.*, 2003, Harth *et al.*, 2005).

Glutamate racemase is known as a druggable enzyme and it has been targeted successfully in inhibitor development programs directed at *S. pneumoniae*, *H. pylori* and *Enterococcus faecalis* (de Dios *et al.*, 2002, Geng *et al.*, 2008, Geng *et al.*, 2009, Fisher, 2008). Recently the crystal structures of MurI from both *M. smegmatis* and *M. tuberculo*sis have been solved and analyzed in comparison to other available MurI structures (Poen *et al.*, 2016), and found to be promising templates for inhibitor development. Another recent report has found the alanine racemase inhibitor, *β*-chloro-D-alanine, binds to and effectively targets mycobacterial MurI (Prosser *et al.*, 2016). Given MurI's essential nature in mycobacteria, and given its track record of yielding potent inhibitors in drug development programs, it could be a promising potential source of new anti-tuberculosis agents.

In many bacteria, MurI is the only source of D-glutamate, but in some bacteria another enzyme, D-amino acid transaminase (D-AAT), can synthesize D-glutamate (Fotheringham *et al.*, 1998). Different combinations of these two enzymes have been reported in various bacterial species. For example, in *B. anthracis* (Oh *et al.*, 2015) and *B. subtilis* (Kimura *et al.*, 2004, Kunst *et al.*, 1997), two isoforms of MurI and a single isoform of D-AAT enzyme are present. In *Listeria monocytogenes* (Majorek KA *et al.*, 2009, Thompson *et al.*, 1998), *Staphylococcus aureus* and *S. haemolyticus* (Pucci, 1995) all three have a MurI and a D-AAT in their genomes. Consistent with recent findings of MurI essentiality, a D-AAT enzyme has not been identified experimentally

or in genomic annotations, in *M. smegmatis*. However, recent proteomic studies have pointed to the possibility of a D-AAT in the mycobacterial genome that could be involved in D-amino acid metabolism, but to date it has not been identified (Halouska *et al.*, 2014, Marshall *et al.*, 2017).

All recent studies support the conditional essentiality of MurI in mycobacteria (Li *et al.*, 2014, Morayya *et al.*, 2015), but it is unknown if its deletion results in a bactericidal or bacteriostatic effect. Further, it is unknown how readily resistance can develop to this deletion (Leekha *et al.*, 2011). To explore the nature of the effect of *murI* deletion on bacterial growth we set up prolonged incubation of D-glutamate auxotrophic Δ*murI* strains in the absence of D-amino acids in an attempt to select for strains with a revertant phenotype (Pankey & Sabath, 2004). Here we report evidence that *murI* deletion in *M. smegmatis* is initially bacteriostatic, and we describe the consistent development of suppressor mutants during prolonged incubation. Further we find that this mutation results in the overexpression of MSMEG_5795, a gene most often annotated as 4-amino-4-deoxychorismate lyase (ADCL) gene, but which we show has D-amino acid transaminase activity.

Results

Isolation and characterization of *murI* suppressor mutants of *M. smegmatis*

Previous work from our group demonstrated that glutamate racemase deletion mutants of *M. smegmatis* mc^2155 were unable to grow in the absence of D-glutamate (Li *et al.*, 2014). To investigate this further, we set up growth experiments in which the incubation period was extended to > 100 h, both in the absence and presence of D-

glutamate (Fig. 1). In the presence of D-glutamate, wild-type and Δ*murI* strains grew to a maximum OD_{600} of approximately 3.5 by about 70 hours (Fig, 1A). In the absence of D-glutamate, the wild-type and genetically complemented Δ*murI* strains grew as before. The Δ*murI* mutant initially failed to grow in the absence of D-glutamate, but prolonged incubation (> 100 h) resulted in eventual growth (Fig. 1B). Cell viability of the Δ*murI* mutant, which was grown without D-glutamate supplementation, was determined and revealed an initial 1-2 log drop in cell count followed by growth recovery beginning at about 80 hours, which by 150 hours was close to wild-type levels (Fig. 1C). Growth curves were repeated (six replicates) with wild-type, *murI* deletion mutants, complemented mutants, and putative suppressor mutants (Fig. 2A). Comparable growth kinetics as observed in Figure 1 were obtained each time. Importantly, the Δ*murI* strain exhibited the same period of non-growth, whereas the suppressor mutants grew like wild-type cultures and did not require re-adaptation to grow in the absence of D-glutamate even following multiple passages of growth in D-glutamate supplemented media (Fig. 2B, C).

Δ*murI* suppressor mutants reveal a consistent genetic change between MSMEG_5795 and 5796

The complete genome sequences of wild-type *M. smegmatis*, Δ*murI* and three putative Δ*murI* suppressor mutants, which we termed S-1, S-2 and S-3, were determined as described in Methods. Initial read mapping to the reference *M. smegmatis* mc²155 (NC_008596) genome identified 130 variations (SNPs and indels). Taking into account these 130 variations, a custom reference genome for our *M. smegmatis* mc²155 strain was then created for the analysis of the suppressor mutant genotypes (Mohan *et al.*, 2015).

DNA Sequence coverage of the *M. smegmatis* genomes averaged 136-fold and is illustrated for the wild-type strain mc²155 (Fig. S1). The presence of the complete *murI* gene in the wild-type strain and the ~540 bp deletion of the *murI* gene in both the Δ*murI* and suppressor mutants is evident in the read coverage. In order to identify the genetic change responsible for the suppressor mutant phenotype, the sequencing data was analyzed to identify the SNPs with the highest variant frequency. SNPs that were present in the three putative Δ*murI* suppressor mutants, but absent in the wild-type or the Δ*murI* mutant are profiled in Table 1 and Table S2. Of these, one SNP mutation, SNP_3, was present in all three putative Δ*murI* suppressor mutants and is found between MSMEG_5795 and MSMEG_5796. Two other SNP mutations were found in two of the putative suppressor mutants and involved either MSMEG_4918 or MSMEG_0516.

SNP_3 is present in the 100 bp intergenic region between MSMEG_5795 and MSMEG_5796. It is not present in the wild-type or Δ*murI* mutant, and consists of a cytosine to thymine (C→T) mutation on the 3'→5' DNA strand 30 nucleotides (nt) upstream of MSMEG_5795. From the perspective of the 5'→3' DNA strand, this SNP would be a guanine to adenine (G→A), change located at 71 nt upstream of MSMEG_5796 (Table 1). In the 100 bp intergenic region, two putative promoter sites were identified. A 5'-TAGAGT-3' consensus promoter sequence was identified 6 nt upstream of MSMEG_5796 gene on the 5'→3' strand in both *M. smegmatis* and *M. tuberculosis* (Fig. 3). This sequence matches with the -10 promoter sequence found for Rv3418c (10kDa/groES) of *M. tuberculosis*, S6 of *M. smegmatis*, and ML0381 (groEL1) of *M. leprae* (Kalate *et al.*, 2003), but is not affected by the SNP identified

here. On the other hand, the SNP_3 change we identified is within a second promoter sequence, 5'-TACGCT-3, which is' located on the 3'→5' DNA strand 26 nt upstream of MSMEG_5795. The SNP results in the sequence becoming 5'-TATGCT-3' (Fig. 3). The 5'-TACGCT-3' promoter sequence is present elsewhere in mycobacteria, for example, at the -10 position of Rv1819c (ABC transporter) in *M. tuberculosis* (Vallecillo & Espitia, 2009) and at the -10 position of the *bla* gene in *M. fortuitum* (Timm *et al.*, 1994b). This promoter sequence is recognized by SigA (Vallecillo & Espitia, 2009).

MSMEG_5795 codes for a protein annotated as 4-amino-4-deoxychorismate lyase (ADCL). This annotation is found in the NCBI, the TBDB (Galagan *et al.*, 2010, Reddy *et al.*, 2009), and MicrobesOnline databases (Dehal *et al.*, 2010), as well as the webTB and SmegmaList databases (Kapopoulou *et al.*, 2011). However, in a minority of cases, it has been annotated additionally as an amino acid transaminase (Dehal *et al.*, 2010). The homolog of MSMEG_5795 in *M. tuberculosis* is Rv0812, and is annotated both as a deoxychorismate lyase and an amino acid aminotransferase in the TBDB and TubercuList databases (Kapopoulou *et al.*, 2011). ADCL catalyzes the PLP dependent conversion of 4-amino-4-deoxychorismate (ADC) to *p*-aminobenzoate and pyruvate (Nakai *et al.*, 2000). This enzyme has been found to be essential in *E. coli* (Green *et al.*, 1992), *Pseudomonas aeruginosa* (Hoang *et al.*, 1998), *Helicobacter pylori* (Salama *et al.*, 2004) and *Acinetobacter baylyi* (de Berardinis *et al.*, 2008) and is involved in folate biosynthesis (O'Rourke *et al.*, 2011). While ADCL does not have a role in D-glutamate synthesis, a type of aminotransferase known as D-amino acid transaminase (D-AAT) is potentially involved in the D-glutamate synthesis pathway as follows: D-alanine + α-ketoglutarate ⇌ pyruvate + D-glutamate (Soda & Esaki, 1985).

Therefore, if MSMEG_5795 is able to function as a D-AAT then SNP_3 could significantly impact D-glutamate synthesis.

MSMEG_5796 encodes a protein that is a part of the glycine cleavage multi-enzyme complex. The complex is present in bacteria and the mitochondria of eukaryotes (Motokawa & Kikuchi, 1971) and catalyzes the formation of N^5, N^{10}-methylenetetrahydrofolate, which is utilized for the biosynthesis of purines, thymidylate, and methionine (Kikuchi *et al.*, 2008). Therefore, this enzyme is unlikely to participate in D-glutamate biosynthesis.

Suppressor mutant strains S-2 and S-3 contain two SNPs in common, but which are unlikely to affect D-glutamate metabolism. For example, they contain a SNP located 859 nt downstream from the translational start site of MSMEG_4918, which codes for a 1,4-alpha-glucan branching enzyme. This SNP is not present in S-1, wild-type or the Δ*murI* mutant (Table 1). S-2 and S-3 contain another SNP located 188 nt downstream from start site of MSMEG_0516, which codes for a protein involved in sugar transport. This change involves a thymine to guanine (T→G) change and is not present in strains S-1, wild-type or Δ*murI* mutant strains (Table 1). As these two genes are unrelated to D-amino acid synthesis or metabolism they would not be likely to affect D-glutamate levels. Notably, a homolog of MSMEG_0516 is not present in *M. tuberculosis*.

SNP_3 significantly increases MSMEG_5795 expression

The effect of SNP_3 on the expression of MSMEG_5795 and MSMEG_5796 was quantified using RT-qPCR. The expression of MSMEG_5795 was found to be 14-fold

higher than wild-type for suppressor mutants 2 and 3, and 3-fold higher for suppressor mutant 1 (Fig. 4A). The changes for suppressor mutants 2 and 3 were statistically significant ($p<0.05$). The expression of MSMEG_5796 was 0.89 to 2.78-fold higher in the Δ*murI* suppressor mutants than in the wild-type strain, but this change was not statistically significant (Fig. 4B). The expression of both these genes in the Δ*murI* mutant was also studied and were not significantly different from wild-type (Fig. 4).

To explore whether the increased expression of MSMEG_5795 in our suppressor mutants was due to increased promoter activity, we monitored the activity of the altered MSMEG_5795 promoter using promoter-*lacZ* fusion constructs created in pJEM15 in *M. smegmatis* mc^2155. All transformed bacteria grew well reaching a maximum OD_{600}=3.0 after about 36 hours. Compared to an empty vector included as a control, the pJEM15 vector containing the wild-type promoter for MSMEG_5795 had measurable promoter activity which gradually increased from about 50 Miller units (MU) in the early exponential phase to about 100 MU in the stationary phase (Fig. 5). Wild-type strains transformed with a construct containing the promoter from Δ*murI* suppressor mutants displayed 150 MU in the early exponential phase followed by an increase to ca. 200 MU in the stationary phase (Fig. 5C), which is roughly 2-fold higher promoter activity than wild-type. These data suggest that the SNP_3 mutation we identified in the promoter leads to significant overexpression of the MSMEG_5795 gene, and is consistent with the RT-qPCR results reported above in which MSMEG_5795 was found to be 14-fold higher in the Δ*murI* suppressor mutants compared to wild-type.

The expression of MSMEG_5795 is insensitive to D-alanine and D-glutamate

The activity of the MSMEG_5795 promoter-*lacZ* fusion constructs was examined for modulation by the cell wall components D-alanine and D-glutamate. The wild-type control MSMEG_5795-*lacZ* fusion construct reached a maximum OD_{600}=3.0 at 36 hours and was found to have 50-100 MU from exponential phase to stationary phase (Fig. 6A). The addition of either 10 mM D-alanine or 10 mM D-glutamate did not significantly alter the MU measurements with 80-100 MU measured over the exponential to stationary phases for the former (Fig. 6B) and 50-90 MU for the latter (Fig. 6C). Interestingly, following the addition of D-alanine, the maximum OD_{600} reached ~3.5 after 40 hours which was slightly higher than the control or the D-glutamate growth curves (Fig. 6).

Strains containing the mutated promoter were examined as above. The MSMEG_5795_SNP_3-*lacZ* fusion construct reached a maximum OD_{600}=3.0 at around 36 hours and its promoter activity was measured from exponential phase to stationary phase at 150-200 MU (Fig. 6D). When this strain was grown following the addition of D-alanine, the promoter activity was measured at 140-180 MU over the exponential to stationary phase of the growth (Fig. 6E). For the cultures containing D-glutamate a trend toward higher promoter activity of 180-220 MU was noted over the exponential to stationary phase of the growth (Fig. 6F). A slightly higher OD_{600} maximum of around 3.5 was again reached for the D-alanine containing culture.

Therefore, wild-type MSMEG_5795 expression does not appear to be modulated by D-alanine and D-glutamate. This is consistent with its promoter being

potentially recognized by SigA factor, which regulates constitutive or housekeeping genes in *Mycobacterium* sp. (Manganelli *et al.*, 2004).

Increased expression of MSMEG_5795 complements both Δ*murI* and Δ*alr* mutants

The ability of MSMEG_5795 to complement the Δ*murI* mutant was investigated further by providing MSMEG_5795 in *trans* under control of the suppressor mutant promoter as well as the wild-type promoter. It was found that providing the gene along with the suppressor mutant promoter was sufficient to complement the Δ*murI* mutant directly, with cultures growing to a maximum OD_{600} ~3.5. This growth is similar to the wild-type strain and to Δ*murI* strains complemented with D-glutamate (Fig. 7A). This result suggests that the MSMEG_5795 gene product is capable of synthesizing D-glutamate directly or stimulating its production.

Providing MSMEG_5795 under control of the wild-type promoter did not initially complement the Δ*murI* strains, but following 55 hours of incubation growth recovery did occur. This period is ~25 hours faster than the 80 hours seen with Δ*murI* mutants (Fig. 7A). The failure to initially complement suggests that the amount of D-glutamate synthesis from the wild-type promoter is insufficient to cause the Δ*murI* revertant phenotype, and that the overexpressing mutation is needed. Also, presumably having a second copy of the MSMEG_5795 gene in the chromosome would increase the chance of an overexpressing mutation involving either of the promoters.

To further analyze the function of the MSMEG_5795 gene product, we introduced it into the Δ*alr* mutant (DM22) that we have previously reported (Milligan

et al., 2007). This strain is auxotrophic for D-alanine and, as expected, the wild-type strain and the D-alanine supplemented Δ*alr* mutant both grow normally and reach their maximum OD_{600} of 3.0 to 3.5 after 30-36 hours. When the Δ*alr* mutant, incubated without D-alanine, was complemented with MSMEG_5795 gene under its native promoter it did not grow. However, when MSMEG_5795 gene was provided in *trans* under control of the suppressor mutant promoter, the Δ*alr* mutant was able to grow, albeit, with an altered growth phenotype requiring 55 hours to reach a maximum OD_{600} of about 2.5 (Fig. 7B).

The MSMEG_5795 protein has significant D-amino acid transaminase activity

To investigate the D-amino acid transaminase activity of the protein product of MSMEG_5795, it was expressed and purified from *M. smegmatis* $mc^2$4517 using immobilized metal affinity and size exclusion chromatography. Using this method, milligram quantities of homogenous protein were produced (Fig. 8A). This protein was assayed for D-AAT activity following a protocol from (Tanizawa *et al.*, 1989, Tanizawa, 1987). Its V_{max} was identified as 13.8 U mg^{-1} and its K_M for D-alanine was 10.2 mM (Fig 8B). In addition, the apparent K_M for pyridoxal phosphate (PLP), which D-AAT is known to use as a co-factor, was found to be 75.4 μM.

The purity of the MSMEG_5795 preparation was confirmed by SDS-PAGE (Fig. 8A) and by liquid chromatography coupled nanospray LTQ-Orbitrap tandem mass spectrometry (LC-MS/MS) of tryptically digested proteins excised from an SDS-PAGE gel band. By using this method, the MSMEG_5795 protein was identified with more than 83% sequence coverage from a heavily loaded central band, as well as in flanking minor bands (see Fig 8A, lane G for a representative Coomassie stained gel).

The upper minor band is predominantly a dimer of MSMEG_5795, but also contains the 60 kDa chaperonin of *M. smegmatis* as a minor contaminant. Very minor signal intensities were detected for other negligible contaminants and none of these additional proteins would suggest a contaminating transaminase activity. As a further check for contaminating proteins that might not stain with Coomassie, we analyzed an in-solution sample of our purified protein using mass spectrometry, as outlined in the updated supplemental material, and again did not identify any protein with contaminating transaminase activity.

To confirm the ability of MSMEG_5795 to produce significant quantities of glutamate from D-alanine, the production of glutamate was confirmed by high resolution mass spectrometry (Fig. 8C). The m/z signal of singly protonated glutamate at 148.06044 was clearly detected with a mass accuracy of less than 0.0001 mass units (Fig. S2 and Fig. S3). The concentration of glutamate increases with incubation time from 0.3 mM at 20 min to 0.7 mM at 40 min and finally to 1.0 mM at 60 min respectively. Additional proof of glutamate production by MSMEG_5795 was obtained by inputting the product of the D-AAT assay as the "substrate" for the coupled glutamate racemase assay which showed time dependent glutamate production (Poen *et al.*, 2016) (Fig. S4).

Lastly, we have also shown that Δ*murI* deletion mutants can be grown in media supplemented with 10 mM D-alanine, for which we observe growth rates and maximum OD_{600} values consistent with wild-type strains (Fig. 9). This result is

consistent with the MSMEG_5795 protein acting via its D-AAT activity, at a substrate value close to its K_M, to produce D-glutamate from D-alanine.

Discussion

The *M. smegmatis ΔmurI* deletion was initially bacteriostatic for growth in the absence of D-glutamate, but prolonged incubation resulted in the generation of suppressor mutants that mapped to the promoter of MSMEG_5795, an uncharacterized gene which is annotated predominately as a 4-amino-4-deoxychorismate lyase (ADCL). Promoter mutations in the suppressor mutants activated the expression of MSMEG_5795 14-fold relative to the wild-type, and these same promoter mutants provided *in trans* were able to complement Δ*murI,* as well as Δ*alr*, mutants.

Biochemical characterization of MSMEG_5795 shows that it has significant D-amino acid transaminase (D-AAT) activity. For example, we have carried out the D-AAT assay using D-alanine and ketoglutarate and determined a clear and significant V_{max} and K_M for this activity. Next, we have taken the output of this assay and shown that it is glutamate using mass spectrometry. We have also shown that this output can serve as input into the glutamate racemase assay. Finally, we show the output of MSMEG_5795, when it is overexpressed, it is able to complement Δ*murI* deletion mutants.

Recently, investigators have predicted the presence of a metabolically important D-AAT enzyme in mycobacteria. This conclusion was based on metabolomic studies that pointed to a shunt from D-glutamate to D-alanine (Marshall

et al., 2017). Potential candidates for genes with D-AAT activity in mycobacteria were explored in these articles, but MSMEG_5795 was not implicated (Halouska *et al.*, 2014). The results of the current study unequivocally establish significant D-AAT activity for the gene product of MSMEG_5795, which we have now shown is capable, in the context of an overexpression mutant, of complementing *murI* deletion and suggest that MSMEG_5795 is the much-sought after mycobacterial D-AAT.

Our findings may have implications for the use of glutamate racemase inhibitors as anti-tuberculosis drugs. The homolog of MSMEG_5795 in *M. tuberculosis* is Rv0812. If Rv0812 codes for a protein with significant D-AAT activity this could mean that glutamate racemase inhibitors would be prone to develop resistance rapidly, via overexpression mutants of Rv0812. However, it is important to be cautious in comparing these two organisms given that their natural habitat, growth characteristics and genetic background are so very different. Also, some bacteria are unable to use their D-AAT genes to rescue D-glutamate auxotrophs. For example, *yheM*, which is the D-AAT gene in *B. subtilis*, does not rescue its D-glutamate auxotroph (Kimura *et al.*, 2004). Also, given that, to avoid the development of resistance, anti-tuberculosis drugs are never given alone, it may be that this will not be an important concern for glutamate racemase inhibitors.

Therapies that target enzymes involved in interdependent aspects of cell wall precursor synthesis, such as glutamate racemase and alanine racemase, or D-AAT and glutamate racemase, might be able to exploit the interrelationships between these enzymes. For example, the revertant is able to synthesize D-glutamate from D-alanine

with D-alanine coming from alanine racemase acting on L-alanine, which is plentiful. However, it is likely that double mutants involving both racemases such as Δ*murI*-Δ*alr* would not be capable of reversion because neither D-alanine or D-glutamate would be available as cell wall precursors, and even a metabolically hyperactive D-AAT would be unable to complement for simultaneously missing both cell wall components. Similarly, double deletion mutants such as, Δ*murI*-ΔMSMEG_5795 would not be able to synthesize D-glutamate for cell wall biosynthesis, even if D-alanine is available. Therefore, drugs targeting a combination of MurI and Alr or MurI and MSMEG_5795 enzymes or all three enzymes could have synergy against tuberculosis. Intriguingly it has been reported by other investigators that, when used against mycobacteria, there is synergy between D-cycloserine and *β*-chloro-D-alanine (David, 2001, Prosser *et al.*, 2016). Perhaps some of this synergy could be due to its action on both of these two racemases, although to be sure the situation is complex given that D-cycloserine itself is targeting at least two enzymes (Prosser & de Carvalho, 2013, Lambert & Neuhaus, 1972, Chacon *et al.*, 2002, Feng & Barletta, 2003).

Finally, while we have shown that MSMEG _5795 functions as a D-AAT enzyme, we have not ruled out that it may also be able to function as ADCL. These two enzymes are closely related. Both enzymes utilize PLP as a co-factor. The active site structure of ADCL is homologous to some transaminases, including D-amino acid transaminases (D-AAT) (Nakai *et al.*, 2000). The ADCL protein in *E. coli* and MSMEG _5795 share 29% identity, higher than the 23% identity shared by the D-amino acid transaminase of *B. subtilis* and MSMEG_5795, which likely explains the predominant

annotation of MSMEG_5795 as an ADCL. Notably, the D-AAT activity we measured for the MSMEG_5795 protein is significant at V_{max} of 13.8 U mg^{-1} but is less than the V_{max} of 200 U mg^{-1} reported for the *Bacillus* enzyme (Van Ophem *et al.*, 1995). This could explain why wild-type MSMEG_5795 under control of its native promoter is unable to rescue Δ*murI* or Δ*alr* deletion strains. Successful complementation requires overexpressing MSMEG_5795 mutants in *M. smegmatis*. This implies that the concentration of substrate or the activity of the enzyme in the wild-type strain is too low to provide sufficient D-glutamate or D-alanine production in Δ*murI* or Δ*alr* mutants respectively. Therefore, it could be that MSMEG_5795 does, in fact, code for ADCL, and that its D-AAT activity is a "moonlighting" function, which for many enzymes is now well recognized (O'Brien & Herschlag, 1999, Khersonsky *et al.*, 2006, Atkins, 2015).

Conclusions

In *M. smegmatis*, we have established that the *murI* gene deletion has a bacteriostatic phenotype which can be rescued by overexpression mutants of MSMEG_5795. We have also shown that MSMEG_5795 is able to act as a D-amino acid transaminase, during the reversion of this phenotype. Therefore, MSMEG_5795 has significant D-AAT activity, in addition to, or instead of its annotated ADCL function. Based on this functional characterization, a revision of the annotation for MSMEG_5795 and its homologs in mycobacteria is recommended. In *M. tuberculosis*, the homolog to MSMEG_5795 is Rv0812. It should be studied to see if it has D-AAT activity which could have an effect on Δ*murI* and Δ*alr* deletion strains.

Experimental Procedures

Bacterial strains, media and growth conditions

All strains and plasmids used in this study are listed in Table 2 or Table S1. Plasmid propagation was carried out in *E. coli* strains, which were grown in Luria-Bertani (LB) medium at 37°C with agitation (220 rpm) or on LB 1.5% agar plates with appropriate antibiotics. Kanamycin was added at 20 μg ml^{-1} for *M. smegmatis*, and 50 μg ml^{-1} for *E. coli*, hygromycin B at 50 μg ml^{-1} for *M. smegmatis,* and 200 μg ml^{-1} for *E. coli*. *Mycobacterium smegmatis* strain mc^2155 (Snapper *et al.*, 1990) and derived strains were maintained on LB agar plates supplemented with 0.05% (w/v) Tween 80 (LBT) with additions as indicated (e.g. 60 mM D-glutamate). For liquid culture, *M. smegmatis* strain mc^2155 was grown at 37°C with agitation [Erlenmeyer flasks (50 ml), 220 rpm] in Hartman's de Bont (HdB) minimal medium (Hartmans & Bont, 1992) supplemented with 0.05% Tween 80 (Sigma Aldrich) and appropriate carbon sources where indicated.

Growth was monitored by optical density measurements at 600 nm (OD_{600}) using culture samples diluted in PBS-Tween 80 to bring OD_{600} to below 0.5 when measured in cuvettes of 1 cm-light path length in an Ultrospec™ 3100 pro (GE Healthcare Life Sciences). Media were inoculated to an initial OD_{600} of 0.001-0.005. Growth rates were determined by plotting the $\log_{10}$ of the OD_{600} versus time. For determination of cell viability (CFU ml^{-1}), the Miles–Misra method was used (Miles *et al.*, 1938). Briefly, the experimental procedure was as follows: Cells pellets from 1 ml culture aliquots were washed with PBS-Tween 80 and resuspended in 1 ml buffer. Ten-fold serial dilutions of 10^{-1} to 10^{-6} were made and 5 μl aliquots were used to

inoculate LBT plates supplemented with 60 mM D-glutamate. For each dilution, four technical replicates were carried out. After inoculation, the plates were incubated at 37˚C for three days.

Isolation and characterization of Δ*murI* suppressor mutants

M. smegmatis Δ*murI* mutants were grown in HdB minimal medium containing 15 mM D-glutamate until an OD_{600} of 0.3 was reached. Cells were harvested by centrifugation and washed with sterile PBS-Tween 80 buffer to remove external D-glutamate. Following resuspension, the cells were used to inoculate fresh growth medium without D-glutamate supplementation to an OD_{600} of approximately 0.001. Cultures were incubated with shaking and Δ*murI* suppressor mutants that grew after ca. 80 hours of incubation at 37˚C were diluted and plated onto LBT agar containing 60 mM D-glutamate. Single colonies of putative suppressor mutants were then tested for their ability to grow on LBT agar plates and in HdB liquid medium without D-glutamate supplementation. Several passages both with and without D-glutamate in the growth medium were used to confirm the suppressor phenotype.

DNA manipulation and whole genome sequencing

All molecular biology techniques were carried out according to standard procedures (Sambrook *et al.*, 1989). Restriction or DNA-modifying enzymes and other molecular biology reagents were obtained from Roche Diagnostics or New England Biolabs. Genomic DNA of *M. smegmatis* (wild-type and mutants) was extracted and purified using an UltraClean® Microbial DNA Isolation kit (MO BIO Laboratories, Inc.) following the manufacturer's instruction. Whole genome sequencing of *M. smegmatis* wild-type and mutants was carried out on an Illumina HiSeq (125 bp paired-end

reads) in the Otago Genomics & Bioinformatics Facility. The reads were assembled by read mapping onto a custom reference genome of *M. smegmatis.* The reads were assembled by mapping to a custom reference genome of *M. smegmatis* and analyzed in fastqc (Andrews, 2010) to show read length, number and quality. Adapter/vector sequences were then removed using BLAST and the UniVec databases. The paired-end reads were then imported into Geneious (Kearse *et al.*, 2012) and run through FLASH (Magoc & Salzberg, 2011) and were then mapped to the reference *M. smegmatis* mc²155 (NC_008596) genome using the read mapper. Polymorphisms in the mapped reads (SNPs and indels) were identified with any variants at 50% frequency or above being added. Exported files were then checked and handled using Geneious and SAMtools (Li *et al.*, 2009), annotated and exported for analysis. The read coverage of the mycobacterial genome was visualized using the Blast Ring Image Generator developed by Scott Beatson's group (Alikhan *et al.*, 2011). The resulting sequencing data were submitted to the NCBI Nucleotide Archive (PRJNA362630).

RNA extraction and reverse transcriptase PCR

Total RNA was extracted using TRIZOL® reagent. Cell lysis was achieved by three cycles of bead beating in a Mini- Beadbeater (Biospec) at 5000 rpm for 30 s. DNA was removed from the RNA preparation by treatment with 2 U RNase-free DNase using the TURBO DNA-free kit (Ambion) according to the manufacturer's instructions. The quality of RNA was checked on a 1% agarose gel and the concentration was determined using a NanoDrop ® ND-1000 spectrophotometer. The Reverse Transcriptase (RT) reactions were carried out using 1 µg of RNA template and gene-specific primers (Table S1). The RT reactions and the quantitative PCR were carried

out using the PrimeScript RT Reagent Kit (Perfect Real Time) (TaKaRa) following manufacturer's instruction with real-time PCR being performed using a LightCycler® 480 System (Roche).

Construction of *lacZ* reporter constructs and complementation of Δ*murI* suppressor mutants.

To study MSMEG_5795 expression, transcriptional fusions of the MSMEG_5795 promoter were cloned into the shuttle vector pJEM15 (Timm *et al.*, 1994a), a plasmid containing a promoterless *lacZ* gene. A 615 bp PCR product encompassing the MSMEG_5795 (-505 to +110) promoter region was amplified from the wild-type strain and from a suppressor mutant (KKRM146) using the primers msDAAT-*lacZ*_FW and msDAAT-*lacZ*_RV (Table 2). The amplified product was cloned into ScaI and BamHI sites of pJEM15. Chemically competent *E. coli* DH10B was transformed with these plasmids via heat shock. Plasmid constructs were extracted and fidelity confirmed using restriction digestion and DNA sequencing before electroporation into *M. smegmatis* mc^2155. The transcriptional activity of the MSMEG_5795 gene was determined using the β-galactosidase assay as described previously by (Gebhard *et al.*, 2006).

For MSMEG_5795 complementation experiments, a region of the MSMEG_5795 gene that comprised -505 bp upstream and +115 bp downstream was amplified (totaling 1490 bp) from both wild-type and Δ*murI* suppressor mutant strains (KKRM146). For this amplification, the msDAAT_NativeP KI_FW and msDAAT_NativeP KI_RV primer pair was used (Table S1). The 1490 bp products were cloned into EcoRV and HindIII sites of the integrating shuttle vector pUHA267 (Table S1). The plasmid constructs

were purified from *E. coli* DH10B and confirmed by restriction digestion and sequencing. Plasmids were electroporated into Δ*murI* and Δ*alr M. smegmatis* mutant strains for downstream phenotypic analysis.

Expression and purification of MSMEG_5795

The open reading frame for MSMEG_5795 (4-amino-4-deoxychorismate lyase) was synthesized with an N-terminal His-tag and a cleavable tobacco etch virus (TEV) protease recognition sequence and inserted into pYUB28b vector (Bashiri *et al.*, 2010) by Genscript (USA). The vector containing the MSMEG_5795 sequence was transformed into *M. smegmatis* $mc^2$4517 cells via electroporation. Cells were grown in Luria-Bertani (LB) Miller Broth containing 0.05% (w/v) Tween 80 and supplemented with 50 μg ml^{-1} kanamycin and 50 μg ml^{-1} hygromycin. Overexpression of MSMEG_5795 was induced with 0.2% (v/v) acetamide at OD_{600} ~0.5, cells were further incubated for 6 hours at 37°C and harvested by centrifugation. Cell pellets were resuspended in 20 mM Tris-HCl pH 7.4, 250 mM sodium chloride, 20 mM imidazole and 0.5 mM pyridoxal 5'-phosphate (PLP) and lysed by sonication. Cell lysate was centrifuged and loaded onto a 5 ml His-Trap™ FF Crude column (GE Healthcare). After removing unbound protein, MSMEG_5795 was eluted by increasing the imidazole concentration to 0.5 M. Fractions with MSMEG_5795 protein were further purified with a HiLoad™ 26/60 Superdex™ 75 prep grade column (GE Healthcare). The gel filtration buffer contained 20 mM Tris-HCl, pH 8.0 and 150 mM NaCl. Purity of samples were assessed with SDS-PAGE and protein concentration was determined using the Coomassie Plus™ Protein Assay reagent (Thermo Fisher).

Biochemical and kinetic analysis of MSMEG_5795

MSMEG_5795 activity was assayed using the coupled enzyme D-amino acid transaminase (D-AAT) assay described by Tanizawa et al. (1987) in which D-alanine and α-ketoglutarate are converted to D-glutamate and pyruvate by D-AAT. Pyruvate is then converted to L-lactate by lactate dehydrogenase coupled to NADH oxidation at 30˚C. The decrease in absorbance at 340 nm was then measured on an Ultrospec™ 3100 pro with SWIFT II software and analyzed using GraphPad Prism version 7.00 for Windows (GraphPad Software, La Jolla California USA). Each reaction mixture contained 100 mM Tris-HCl pH 8.1, 10 mM α-ketoglutarate, 0.15 mM PLP, 5 U L-lactate dehydrogenase and 0.2 mM NADH. The enzyme concentration used for the assays was 77 nM. Each reaction mix was pre-incubated at 30°C for 5 minutes and the absorbance at 340 nm was measured for 2 minutes to set a baseline. The reaction was started by adding various concentration of D-alanine (25.0, 12.5, 6.25, 3.13, 1.57, 0.78, and 0.39 and 0.20 mM) to the assay mix and rates were measured for 30 minutes at 30 °C. To determine the apparent K_M of D-AAT for PLP, the enzyme and D-alanine concentration were fixed to 77 nM and 25 mM, respectively. Assays were performed as described above in the presence of different concentrations (400, 200, 100, 50,1 and 0 µM) of the PLP cofactor .

Mass spectrometry detection of glutamate produced by MSMEG_5795

The formation of glutamate by MSMEG_5795 was directly determined by high resolution orbitrap mass spectrometry by assaying only the first reaction of the coupled D-AAT assay following protein removal (see description next paragraph). The first reaction of coupled D-AAT assay was performed with concentrations of

MSMEG_5795 of 77 nM and D-alanine of 25 mM. All other components required for the first reaction were added as described above. The reaction mixtures were incubated for 20, 40 and 60 min. The negative control contained water instead of D-alanine and was incubated for 60 minutes. All reactions were performed in duplicate. Following incubation, the reaction mixtures were filtered through an ultrafiltration membrane with a molecular weight cut-off of 10 kDa to remove the MSMEG_5795 protein. One µl of each filtrate (containing the low molecular weight compounds) was diluted with 98 µl of 5% acetonitrile and 0.2% formic acid in water (solvent A) and supplemented with 1 µl of 10 mM aspartate as a reference compound. Five µl of each sample were then injected by direct infusion into a nanospray coupled LTQ-Orbitrap XL mass spectrometer (Thermo Scientific, San Jose, CA) at a flow rate of 800 nl of solvent A per min. All mass measurements were performed in the orbitrap mass analyser at a resolution of 100,000 at m/z 400. Every full MS scan in the mass range of m/z 125-180 was followed by two pseudo selected reaction monitoring (pSRM) measurements of m/z 134.045 (singly protonated aspartate) and 148.060 (singly protonated glutamate). The isolation window for precursor selection was set to 3 Da and the normalized collision energy was kept at 0 to allow for an intact precursor ion measurement in the orbitrap. The relative amount of glutamate was measured as the ratio of the glutamate peak intensity versus the peak intensity of the constant amount of spiked aspartate to compensate for fluctuations in ionization and sample interferences. For the determination of the concentration of glutamate in the reaction mix an external standard curve of increasing glutamate concentrations at a constant aspartate concentration was prepared as described in Fig. S2.

Glutamate racemase assay detection of glutamate from MSMEG_5795

To detect the D-glutamate production by MSMEG_5795, the first step of D-AAT assay was performed as described above for the characterization of MSMEG_5795. Each assay contained 77 nM MSMEG_5795 and 25 mM D-alanine. For this experiment, the absorbance was monitored at 340 nm for 20, 40 and 60 minutes; each assay was performed in duplicate. The negative control contained water instead of D-alanine and was assayed for 60 minutes. Each reaction was stopped by transferring the reactions to 4°C. MSMEG_5795 and L-LDH, were removed immediately using an ultrafiltration membrane (Vivaspin2 with 10 kDa MWCO, GE Healthcare), and the protein free filtrate was utilized for subsequent analysis by mass spectrometry.

The protein-free output of the D-AAT assay was also used as substrate for the glutamate racemase (MurI) activity to show that it contained significant quantities of glutamate. The MurI assay was performed as previously described by Poen *et al*. (2016). Each 1 ml assay mix contained 50 mM CHES (N-Cyclohexyl-2-aminoethanesulfonic acid) pH 9.2, 5 mM nicotinamide adenine dinucleotide, 37.5 U ml^{-1} L-glutamate dehydrogenase, 2.5 mM adenosine 5'-diphosphate, 0.65 mM iodonitrotetrazolium chloride), 2 U ml^{-1} diaphorase. The reaction was initiated by the addition of glutamate racemase from *B. anthracis* to a final concentration of 10 µM, and contained 100 µl of the D-AAT assay output as substrate. The absorbance was monitored at 500 nm on an Ultrospec™ 3100 pro with SWIFT II software for 30 minutes at 30°C. The negative control contained water instead of substrate.

Acknowledgements

This research was supported by a doctoral scholarship from the University of Otago to R. M., the Maurice Wilkins Centre at the University of Auckland, The Thrash Foundation, Houston, Texas and Lottery Health Research New Zealand – LHR2017-48905. The authors would also like to thank the Otago Genomics & Bioinformatics Facility, for next generation sequencing and the Centre for Protein Research, for mass spectrometry, both at the University of Otago.

Author contributions

RM, HTA, GT, HKOR and TK carried out the experiments and wrote the paper. GMC and KLK proposed the study, contributed to experiment design, and revised the manuscript. All authors read and approved the final manuscript.

Conflicts of Interest

K. L. K. and H. K. O. R have received funding for alanine racemase related projects from L2 Diagnostics LLC, New Haven, Conn.

Supporting information

Additional supporting information may be found in the online version of this article.

References

Alikhan, N.-F., N.K. Petty, N.L. Ben Zakour & S.A. Beatson, (2011) BLAST Ring Image Generator (BRIG): simple prokaryote genome comparisons. *BMC Genomics* **12**: 1-10.

Andrews, S., (2010) Babraham Bioinformatics - FastQC A Quality Control tool for High Throughput Sequence Data. Available online at: http://www.bioinformatics.babraham.ac.uk/projects/fastqc.

Atkins, W.M., (2015) Biological messiness vs. biological genius: Mechanistic aspects and roles of protein promiscuity. *The Journal of steroid biochemistry and molecular biology* **151**: 3-11.

Bashiri, G., A.M. Rehan, D.R. Greenwood, J.M. Dickson & E.N. Baker, (2010) Metabolic engineering of cofactor F420 production in *Mycobacterium smegmatis*. *PLoS ONE* **5**: e15803.

Chacon, O., Z. Feng, N.B. Harris, N.E. Cáceres, L.G. Adams & R.G. Barletta, (2002) *Mycobacterium smegmatis* D-Alanine Racemase Mutants Are Not Dependent on D-Alanine for Growth. *Antimicrob Agents Chemother* **46**: 47-54.

David, S., (2001) Synergic activity of D-cycloserine and *β*-chloro-D-alanine against *Mycobacterium tuberculosis*. *J Antimicrob Chemother* **47**: 203-206.

de Berardinis, V., D. Vallenet, V. Castelli, M. Besnard, A. Pinet, C. Cruaud, S. Samair, C. Lechaplais, G. Gyapay, C. Richez, M. Durot, A. Kreimeyer, F. Le Fevre, V. Schachter, V. Pezo, V. Doring, C. Scarpelli, C. Medigue, G.N. Cohen, P. Marliere, M. Salanoubat & J. Weissenbach, (2008) A complete collection of single-gene deletion mutants of *Acinetobacter baylyi* ADP1. *Molecular systems biology* **4**: 174.

de Dios, A., L. Prieto, J.A. Martin, A. Rubio, J. Ezquerra, M. Tebbe, B. Lopez de Uralde, J. Martin, A. Sanchez, D.L. LeTourneau, J.E. McGee, C. Boylan, T.R. Parr, Jr. & M.C. Smith, (2002) 4-Substituted D-glutamic acid analogues: the first potent inhibitors of glutamate racemase (MurI) enzyme with antibacterial activity. *Journal of medicinal chemistry* **45**: 4559-4570.

Dehal, P.S., M.P. Joachimiak, M.N. Price, J.T. Bates, J.K. Baumohl, D. Chivian, G.D. Friedland, K.H. Huang, K. Keller, P.S. Novichkov, I.L. Dubchak, E.J. Alm & A.P. Arkin, (2010) MicrobesOnline: an integrated portal for comparative and functional genomics. *Nucleic Acids Res* **38**: D396-400.

Dheda, K., T. Gumbo, N.R. Gandhi, M. Murray, G. Theron, Z. Udwadia, G.B. Migliori & R. Warren, (2014) Global control of tuberculosis: from extensively drug-resistant to untreatable tuberculosis. *The Lancet. Respiratory medicine* **2**: 321-338.

Doublet, P., J. van Heijenoort, J.P. Bohin & D. Mengin-Lecreulx, (1993) The *murI* gene of *Escherichia coli* is an essential gene that encodes a glutamate racemase activity. *J Bacteriol* **175**: 2970-2979.

Feng, Z. & R.G. Barletta, (2003) Roles of Mycobacterium smegmatis D-alanine:D-alanine ligase and D-alanine racemase in the mechanisms of action of and resistance to the peptidoglycan inhibitor D-cycloserine. *Antimicrob Agents Chemother* **47**: 283-291.

Fisher, S.L., (2008) Glutamate racemase as a target for drug discovery. *Microbial biotechnology* **1**: 345-360.

Fotheringham, I.G., S.A. Bledig & P.P. Taylor, (1998) Characterization of the genes encoding D-amino acid transaminase and glutamate racemase, two D-glutamate biosynthetic enzymes of *Bacillus sphaericus* ATCC 10208. *J Bacteriol* **180**: 4319-4323.

Galagan, J.E., P. Sisk, C. Stolte, B. Weiner, M. Koehrsen, F. Wymore, T.B. Reddy, J.D. Zucker, R. Engels, M. Gellesch, J. Hubble, H. Jin, L. Larson, M. Mao, M. Nitzberg, J. White, Z.K. Zachariah, G. Sherlock, C.A. Ball & G.K. Schoolnik, (2010) TB database 2010: overview and update. *Tuberculosis (Edinb)* **90**: 225-235.

Gandhi, N.R., J.R. Andrews, J.C. Brust, R. Montreuil, D. Weissman, M. Heo, A.P. Moll, G.H. Friedland & N.S. Shah, (2012) Risk factors for mortality among MDR- and XDR-TB patients in

a high HIV prevalence setting. *The international journal of tuberculosis and lung disease : the official journal of the International Union against Tuberculosis and Lung Disease* **16**: 90-97.

Gebhard, S., S.L. Tran & G.M. Cook, (2006) The Phn system of *Mycobacterium smegmatis*: a second high-affinity ABC-transporter for phosphate. *Microbiology* **152**: 3453-3465.

Geng, B., G. Basarab, J. Comita-Prevoir, M. Gowravaram, P. Hill, A. Kiely, J. Loch, L. MacPherson, M. Morningstar, G. Mullen, E. Osimboni, A. Satz, C. Eyermann & T. Lundqvist, (2009) Potent and selective inhibitors of *Helicobacter pylori* glutamate racemase (MurI): pyridodiazepine amines. *Bioorganic & medicinal chemistry letters* **19**: 930-936.

Geng, B., G. Breault, J. Comita-Prevoir, R. Petrichko, C. Eyermann, T. Lundqvist, P. Doig, E. Gorseth & B. Noonan, (2008) Exploring 9-benzyl purines as inhibitors of glutamate racemase (MurI) in Gram-positive bacteria. *Bioorganic & medicinal chemistry letters* **18**: 4368-4372.

Grant, S.G., J. Jessee, F.R. Bloom & D. Hanahan, (1990) Differential plasmid rescue from transgenic mouse DNAs into *Escherichia coli* methylation-restriction mutants. *Proc Natl Acad Sci U S A* **87**: 4645-4649.

Green, J.M., W.K. Merkel & B.P. Nichols, (1992) Characterization and sequence of *Escherichia coli* pabC, the gene encoding aminodeoxychorismate lyase, a pyridoxal phosphate-containing enzyme. *Journal of Bacteriology* **174**: 5317-5323.

Griffin, J.E., J.D. Gawronski, M.A. Dejesus, T.R. Ioerger, B.J. Akerley & C.M. Sassetti, (2011) High-resolution phenotypic profiling defines genes essential for mycobacterial growth and cholesterol catabolism. *PLoS pathogens* **7**: e1002251.

Halouska, S., R.J. Fenton, D.K. Zinniel, D.D. Marshall, R.G. Barletta & R. Powers, (2014) Metabolomics analysis identifies D-Alanine-D-Alanine ligase as the primary lethal target of D-Cycloserine in mycobacteria. *Journal of proteome research* **13**: 1065-1076.

Harth, G., S. Maslesa-Galic, M.V. Tullius & M.A. Horwitz, (2005) All four *Mycobacterium tuberculosis* glnA genes encode glutamine synthetase activities but only GlnA1 is abundantly expressed and essential for bacterial homeostasis. *Mol Microbiol* **58**: 1157-1172.

Hartmans, S. & d.J.A.M. Bont, (1992) The genus Mycobacterium-nonmedical. *In: The Prokaryotes, A. Balows et al.(eds.). 2nd Ed.* Springer Verlag, New York (1992) 1214-1237.

Hoang, T.T., R.R. Karkhoff-Schweizer, A.J. Kutchma & H.P. Schweizer, (1998) A broad-host-range Flp-FRT recombination system for site-specific excision of chromosomally-located DNA sequences: application for isolation of unmarked *Pseudomonas aeruginosa* mutants. *Gene* **212**: 77-86.

Kalate, R.N., S.S. Tambe & B.D. Kulkarni, (2003) Artificial neural networks for prediction of mycobacterial promoter sequences. *Computational biology and chemistry* **27**: 555-564.

Kapopoulou, A., J.M. Lew & S.T. Cole, (2011) The MycoBrowser portal: A comprehensive and manually annotated resource for mycobacterial genomes. *Tuberculosis* **91**: 8-13.

Kearse, M., R. Moir, A. Wilson, S. Stones-Havas, M. Cheung, S. Sturrock, S. Buxton, A. Cooper, S. Markowitz, C. Duran, T. Thierer, B. Ashton, P. Meintjes & A. Drummond, (2012) Geneious Basic: an integrated and extendable desktop software platform for the organization and analysis of sequence data. *Bioinformatics* **28**: 1647-1649.

Khersonsky, O., C. Roodveldt & D.S. Tawfik, (2006) Enzyme promiscuity: evolutionary and mechanistic aspects. *Current opinion in chemical biology* **10**: 498-508.

Kikuchi, G., Y. Motokawa, T. Yoshida & K. Hiraga, (2008) Glycine cleavage system: reaction mechanism, physiological significance, and hyperglycinemia. *Proceedings of the Japan Academy. Series B, Physical and biological sciences* **84**: 246-263.

Kimura, K., L.S. Tran & Y. Itoh, (2004) Roles and regulation of the glutamate racemase isogenes, *racE* and *yrpC*, in *Bacillus subtilis*. *Microbiology* **150**: 2911-2920.

Kunst, F., N. Ogasawara, I. Moszer, A.M. Albertini, G. Alloni, V. Azevedo, M.G. Bertero, P. Bessieres, A. Bolotin, S. Borchert, R. Borriss, L. Boursier, A. Brans, M. Braun, S.C. Brignell, S. Bron, S. Brouillet, C.V. Bruschi, B. Caldwell, V. Capuano, N.M. Carter, S.K. Choi, J.J. Codani, I.F. Connerton, A. Danchin & et al., (1997) The complete genome sequence of the gram-positive bacterium *Bacillus subtilis*. *Nature* **390**: 249-256.

Lambert, M.P. & F.C. Neuhaus, (1972) Mechanism of D-cycloserine action: alanine racemase from *Escherichia coli* W. *J Bacteriol* **110**: 978-987.

Leekha, S., C.L. Terrell & R.S. Edson, (2011) General Principles of Antimicrobial Therapy. *Mayo Clinic Proceedings* **86**: 156-167.

Li, H., B. Handsaker, A. Wysoker, T. Fennell, J. Ruan, N. Homer, G. Marth, G. Abecasis & R. Durbin, (2009) The Sequence Alignment/Map format and SAMtools. *Bioinformatics* **25**: 2078-2079.

Li, Y., R. Mortuza, D.L. Milligan, S.L. Tran, U. Strych, G.M. Cook & K.L. Krause, (2014) Investigation of the essentiality of glutamate racemase in *Mycobacterium smegmatis*. *J Bacteriol* **196**: 4239-4244.

Lundqvist, T., S.L. Fisher, G. Kern, R.H. Folmer, Y. Xue, D.T. Newton, T.A. Keating, R.A. Alm & B.L. de Jonge, (2007) Exploitation of structural and regulatory diversity in glutamate racemases. *Nature* **447**: 817-822.

Magoc, T. & S.L. Salzberg, (2011) FLASH: fast length adjustment of short reads to improve genome assemblies. *Bioinformatics* **27**: 2957-2963.

Majorek KA, Chruszcz M, Skarina T, Onopriyenko O, Stam J, Anderson WF, Savchenko A, Bujnicki JM & M. W, (2009) Crystal structure of glutamate racemase from *Listeria monocytogenes* in complex with succinic acid. In. RCSB PDB, http://www.rcsb.org/pdb/explore/explore.do?structureId=3IST.

Manganelli, R., R. Provvedi, S. Rodrigue, J. Beaucher, L. Gaudreau & I. Smith, (2004) Sigma factors and global gene regulation in *Mycobacterium tuberculosis*. *J Bacteriol* **186**: 895-902.

Marshall, D.D., S. Halouska, D.K. Zinniel, R.J. Fenton, K. Kenealy, H.K. Chahal, G. Rathnaiah, R.G. Barletta & R. Powers, (2017) Assessment of Metabolic Changes in *Mycobacterium smegmatis* Wild-Type and alr Mutant Strains: Evidence of a New Pathway of D-Alanine Biosynthesis. *Journal of proteome research* **16**: 1270-1279.

Miles, A.A., S.S. Misra & J.O. Irwin, (1938) The estimation of the bactericidal power of the blood. *The Journal of hygiene* **38**: 732-749.

Milligan, D.L., S.L. Tran, U. Strych, G.M. Cook & K.L. Krause, (2007) The alanine racemase of *Mycobacterium smegmatis* is essential for growth in the absence of D-alanine. *J Bacteriol* **189**: 8381-8386.

Mohan, A., J. Padiadpu, P. Baloni & N. Chandra, (2015) Complete Genome Sequences of a *Mycobacterium smegmatis* Laboratory Strain (MC2 155) and Isoniazid-Resistant (4XR1/R2) Mutant Strains. *Genome announcements* **3**:10.1128/genomeA.01520-14

Morayya, S., D. Awasthy, R. Yadav, A. Ambady & U. Sharma, (2015) Revisiting the essentiality of glutamate racemase in *Mycobacterium tuberculosis*. *Gene* **555**: 269-276.

Motokawa, Y. & G. Kikuchi, (1971) Glycine metabolism in rat liver mitochondria. V. Intramitochondrial localization of the reversible glycine cleavage system and serine hydroxymethyltransferase. *Arch Biochem Biophys* **146**: 461-464.

Nakai, T., H. Mizutani, I. Miyahara, K. Hirotsu, S. Takeda, K.H. Jhee, T. Yoshimura & N. Esaki, (2000) Three-dimensional structure of 4-amino-4-deoxychorismate lyase from *Escherichia coli*. *Journal of biochemistry* **128**: 29-38.

O'Brien, P.J. & D. Herschlag, (1999) Catalytic promiscuity and the evolution of new enzymatic activities. *Chemistry & biology* **6**: R91-R105.

O'Rourke, P.E., T.C. Eadsforth, P.K. Fyfe, S.M. Shepherd & W.N. Hunter, (2011) *Pseudomonas aeruginosa* 4-amino-4-deoxychorismate lyase: spatial conservation of an active site tyrosine and classification of two types of enzyme. *PLoS ONE* **6**: e24158.

Oh, S.Y., S.G. Richter, D.M. Missiakas & O. Schneewind, (2015) Glutamate Racemase Mutants of *Bacillus anthracis*. *J Bacteriol* **197**: 1854-1861.

Pankey, G.A. & L.D. Sabath, (2004) Clinical Relevance of Bacteriostatic versus Bactericidal Mechanisms of Action in the Treatment of Gram-Positive Bacterial Infections. *Clinical Infectious Diseases* **38**: 864-870.

Poen, S., Y. Nakatani, H.K. Opel-Reading, M. Lasse, R.C. Dobson & K.L. Krause, (2016) Exploring the structure of glutamate racemase from *Mycobacterium tuberculosis* as a template for anti-mycobacterial drug discovery. *Biochem J* **473**: 1267-1280.

Prosser, G.A. & L.P. de Carvalho, (2013) Metabolomics Reveal D-Alanine:D-Alanine Ligase As the Target of D-Cycloserine in *Mycobacterium tuberculosis*. *ACS Med Chem Lett* **4**: 1233-1237.

Prosser, G.A., A. Rodenburg, H. Khoury, C. de Chiara, S. Howell, A.P. Snijders & L.P. de Carvalho, (2016) Glutamate Racemase Is the Primary Target of beta-Chloro-D-Alanine in *Mycobacterium tuberculosis*. *Antimicrob Agents Chemother* **60**: 6091-6099.

Pucci, M.J., J. A. Thanassi, H. T. Ho, P. J. Falk, and T. J. Dougherty., (1995) *Staphylococcus haemolyticus* contains two D-glutamic acid biosynthetic activities, a glutamate racemase and a D-amino acid transaminase. *J Bacteriol.* **177**: 336-342.

Reddy, T.B., R. Riley, F. Wymore, P. Montgomery, D. DeCaprio, R. Engels, M. Gellesch, J. Hubble, D. Jen, H. Jin, M. Koehrsen, L. Larson, M. Mao, M. Nitzberg, P. Sisk, C. Stolte, B. Weiner, J. White, Z.K. Zachariah, G. Sherlock, J.E. Galagan, C.A. Ball & G.K. Schoolnik, (2009) TB database: an integrated platform for tuberculosis research. *Nucleic Acids Res* **37**: D499-508.

Salama, N.R., B. Shepherd & S. Falkow, (2004) Global Transposon Mutagenesis and Essential Gene Analysis of *Helicobacter pylori*. *Journal of Bacteriology* **186**: 7926-7935.

Sambrook, J., E.F. Fritsch & T. Maniatis, (1989) *Molecular Cloning: A Laboratory Manual, 2nd ed.* Cold Spring Harbor Laboratory Press, Cold Spring Harbor, NY.

Sassetti, C.M., D.H. Boyd & E.J. Rubin, (2003) Genes required for mycobacterial growth defined by high density mutagenesis. *Mol Microbiol* **48**: 77-84.

Snapper, S.B., R.E. Melton, S. Mustafa, T. Kieser & W.R. Jacobs, Jr., (1990) Isolation and characterization of efficient plasmid transformation mutants of *Mycobacterium smegmatis*. *Mol Microbiol* **4**: 1911-1919.

Soda, K. & N. Esaki, (1985) D-Amino acid transaminase. In: Transaminases. P. Christen & D.E. Metzler (eds). New York, N.Y.: John Wiley & Sons, Inc., pp. 463–467.

Tanizawa, K., Y. Masu, S. Asano, H. Tanaka & K. Soda, (1989) Thermostable D-amino acid aminotransferase from a thermophilic *Bacillus* species. Purification, characterization, and active site sequence determination. *J Biol Chem* **264**: 2445-2449.

Tanizawa, K., Masu, Y., Asano, S., Tanaka, H., Soda, K., (1987) D-Amino Acid Aminotransferase from a Thermophile, YM-1: enzymological properties, cloning of the amino acid sequence. In:

The 7th International Congress on Chemical and Biological Aspects of Vitamin B6 Catalysis. T. Korpela, and Christen, P. (ed). Turku, Finland Birkhauser Verlag, pp. 43-46.

Thompson, R.J., H.G.A. Bouwer, D.A. Portnoy & F.R. Frankel, (1998) Pathogenicity and immunogenicity of a *Listeria monocytogenes* strain that requires D-alanine for growth. *Infection and Immunity* **66**: 3552-3561.

Timm, J., E.M. Lim & B. Gicquel, (1994a) *Escherichia coli*-mycobacteria shuttle vectors for operon and gene fusions to lacZ: the pJEM series. *J Bacteriol* **176**: 6749-6753.

Timm, J., M.G. Perilli, C. Duez, J. Trias, G. Orefici, L. Fattorini, G. Amicosante, A. Oratore, B. Joris, J.M. Frere & et al., (1994b) Transcription and expression analysis, using lacZ and phoA gene fusions, of *Mycobacterium fortuitum* beta-lactamase genes cloned from a natural isolate and a high-level beta-lactamase producer. *Mol Microbiol* **12**: 491-504.

Vallecillo, A.J. & C. Espitia, (2009) Expression of *Mycobacterium tuberculosis* pe_pgrs33 is repressed during stationary phase and stress conditions, and its transcription is mediated by sigma factor A. *Microbial pathogenesis* **46**: 119-127.

Van Ophem, P.W., M.A. Pospischil, D. Ringe, D. Peisach, G. Petsko, K. Soda & J.M. Manning, (1995) Catalytic ability and stability of two recombinant mutants of D-amino acid transaminase involved in coenzyme binding. *Protein Sci* **4**: 2578-2586.

WHO, (2015) Global tuberculosis report. In.: World Health Organization, http://www.who.int/tb/publications/global_report/en/.

WHO, (2017) Drug resistant TB. In.: World Health Organization, http://www.who.int/tb/areas-of-work/drug-resistant-tb/en/.

Tables

Table 1: Summary of the SNP analysis from the whole genome sequencing

	SNP_1	**SNP_2**	**SNP_3**
	MSMEG_4918 (glucan branching enzyme)	MSMEG_0516 (sugar transport)	Between MSMEG_5795 (deoxychorismate lyase) and MSMEG_5796 (glycine cleavage MEC)
Strain containing SNP	S-2, S-3	S-2, S-3	S-1, S-2, S-3
Base change in SNP	G→A	T→G	C→T (or, G→A)
Amino acid (a.a.) changes	Val 287→Ile	Val 63 → Gly	NA
SNP distance from start codon in nucleotides (nt)	859 nt	188 nt	30 nt from 5795
Gene orientation	(+)	(+)	(-)
Gene length	2211 bp	912 bp	870 bp
M. tuberculosis homologue	Rv1326c	no homologue	Rv0812

Table 2: Bacterial strains, plasmids and primers used in this study

Strain or plasmid	Description*	Reference and source
Escherichia coli strains		
DH10B	F⁻ *araD139* Δ(*ara*, *leu*)*7697* Δ*lacX74 galU galK rpsL deoR Φ*80d*lacZ* ΔM15 *endA1 nupG recA1 mcrA* Δ(*mrr hsdRMS mcrBC*)	(Grant *et al.*, 1990)
Mycobacterium smegmatis strains		
mc^2155 wild-type	Efficient plasmid transformation (Ept) phenotype	(Snapper *et al.*, 1990)
DM22	mc^2155 Δ*alr*::*aphA-3* Kan^r	(Milligan *et al.*, 2007)
KK104-10 (DM104)	mc^2155 Δ*murI*::*aphA-3* Kan^r; selected at 60 mM D-glutamate	(Li *et al.*, 2014)
KKRM134	DM104 Revertant-1	This study
KKRM146	DM104 Revertant-2	″
KKRM147	DM104 Revertant-3	″
Plasmids		
pJEM15	*E. coli-Mycobacterium* shuttle vector for the creation of transcriptional promoter fusions to *lacZ*, Kan^r	(Timm *et al.*, 1994b)
pUHA267	*E. coli-Mycobacterium* shuttle vector with mycobacteriophage L5 integrase and *attP* for integration into *attB* of *Mycobacteria*; Hyg^r	AgResearch, Wallaceville, New Zealand
pYUB28b	*Mycobacteria* shuttle vector for protein expression; Hyg^r	(Bashiri *et al*., 2010)

*Kan^r, kanamycin resistance; Hyg^r, hygromycin resistance

Figure Legends

Figure 1: Growth curves and cell viability curves for *M. smegmatis* Δ*murI* strains

Growth curves for *M. smegmatis* mc²155-Otago (wild-type) (black curve), Δ*murI* (brown curve) and *murI* complemented Δ*murI* (green curve) strains. For (A) and (B) the x-axis represents hours of incubation and the y-axis represents the OD_{600} of the cultures. For (C) CFU ml^{-1} is plotted on the y-axis. The arrows indicates the point at which the inoculum was washed and new medium was introduced. Error bars represent one standard deviation.

(A) Growth curves in D-glutamate supplemented minimal medium.

(B) Growth curves in minimal medium without D-glutamate supplementation.

(C) Colony counts strains from the cultures shown in (B).

Figure 2: Stable phenotype of putative suppressors derived from the Δ*murI* strains

(A) Growth phenotype of wild-type (black curve), Δ*murI* (brown curve), Δ*murI* (fresh culture from glycerol stock) (maroon curve), putative Δ*murI* suppressor (orange curve) and *murI* complemented (green curve) in minimal medium. Here, the x-axis represents incubation hours and the y-axis represents OD_{600} of the cultures. The black arrow indicates the point at which the inoculum was washed and new medium was inoculated. Error bars represent one standard deviation here and in panel B and C.

(B) The growth of wild-type (black curve) and putative Δ*murI* suppressors (orange curve) in minimal medium grown without D-glutamate supplementation. Incubation hours and OD_{600} of the culture are plotted on the x-axis and y-axis respectively.

(C) Growth curves of putative Δ*murI* suppressor strains grown for 10 passages in minimal medium in the presence of D-glutamate. In the graph, incubation hours are plotted on the x-axis and OD_{600} of the culture is plotted on the y-axis. Each black growth curve represents one passage. Additional cultures of the fourth, seventh, and tenth passages grown *without* D-glutamate supplementation are shown as red growth curves.

Figure 3: Gene organization of 4-amino-4-deoxychorismate lyase (MSMEG_5795)

The brown arrow represents MSMEG_5794 gene. The blue arrow represents MSMEG_5795 gene. The pink arrow represents MSMEG_5796. The green arrow represents MSMEG_5797. The numbers above the intergenic junctions represent the distance between genes. The position of SNP_3 is highlighted in yellow. The direction of the arrow indicates the direction of transcription of the gene. Box 1 shows the location of a consensus promoter sequence 12 nucleotides upstream of the translational start site of MSMEG_5796 gene. Box 2 shows the consensus promoter sequence 26 nucleotides upstream of the start codon of the MSMEG_5795 gene. The bold black arrow near Box 2 points to the SNP in front of MSMEG_5795 that leads to its increased expression.

Figure 4: RT-qPCR of MSMEG_5795 and MSMEG_5796 genes

RT-qPCR data for wild-type, Δ*murI*, and putative suppressor Δ*murI* strains S-1, S-2 and S-3. The target/reference ratio is plotted on the y-axis where '*' indicates statistical significance at $P<0.05$. Error bars represent one standard deviation. Table underneath presents the fold change in gene expression. (A) Data for MSMEG_5795 (B) Data for MSMEG_5796.

Figure 5: Promoter activity in the upstream region of MSMEG_5795

The activity of promoter-*lacZ* fusion constructs, as described in the text, embedded in a pJEM15 vector in *M. smegmatis* is plotted at various points on a growth curve. The growth progression of *M. smegmatis* mc²155-Otago (wild-type) is shown as a line drawing with black circles indicating the OD_{600} on the left y-axis. The promoter activity is plotted as black bars reflecting Miller Units according to the scale on the right y-axis. Hour of incubation is plotted along the x-axis. Error bars represent one standard deviation.

(A) Growth progression and MSMEG_5795-*lacZ* activity of wild-type *M. smegmatis* mc²155-Otago strain containing an empty pJEM15 plasmid

(B) Growth progression and MSMEG_5795-*lacZ* activity of wild-type *M. smegmatis* mc²155-Otago strain containing the wild-type MSMEG_5795 promoter on a pJEM15 plasmid

(C) The growth curve and MSMEG_5795-*lacZ* activity of wild-type *M. smegmatis* mc²155-Otago strain containing the SNP_3 promoter sequence for MSMEG_5795 on a pJEM15 plasmid

Figure 6: Promoter activity in the presence of D-alanine and D-glutamate

The activity of promoter-*lacZ* fusion constructs in a pJEM15 vector as affected by D-alanine and D-glutamate is plotted at various points on a growth curve. The growth progression of *M. smegmatis* mc²155-Otago (wild-type) is shown as a line drawing with black circles indicating the OD_{600} on the left y-axis. The promoter activity is plotted as black bars reflecting Miller Units according to the scale on the right y-axis. Hour of incubation is plotted along the x-axis. Error bars represent one standard deviation.

(A) The growth and LacZ activity of the *M. smegmatis* mc²155-Otago (wild-type) strain transformed with the wild-type promoter coupled to a MSMEG_5795-*lacZ* construct.

(B) as in (A) but grown with supplemental 10 mM D-alanine or (C) 10 mM D-glutamate.

(D) The growth and LacZ activity of wild-type *M. smegmatis* transformed with a pJEM15 vector containing the SNP_3 promoter sequence coupled to a MSMEG_5795-*lacZ* construct.

(E) as in (D) but grown with supplemental 10 mM D-alanine or (F) 10 mM D-glutamate.

Figure 7: Growth profiles of wild type, Δ*murI* and Δ*alr* strains complemented with MSMEG_5795, D-alanine or D-glutamate

(A) Growth curves of wild-type mc²155 (●), Δ*murI* (Δ, green) supplemented with 15 mM D-glutamate, Δ*murI* complemented with MSMEG_5795 driven by the SNP_3 containing promoter (◇, red), Δ*murI* without D-glutamate supplementation (▼, brown), Δ*murI* containing the empty vector pUHA267 (▽, green yellow), and Δ*murI* complemented with MSMEG_5795 driven by the wild-type promoter (◆, blue).

(B) Growth curves of wild-type mc²155 (●), Δ*alr* (Δ, green) supplemented with 10 mM D-glutamate, Δ*alr*, without D-alanine supplementation, complemented with MSMEG_5795 driven by the SNP_3 containing promoter (◇, red), Δ*alr* without D-alanine supplementation (▼, brown), Δ*alr* containing the empty vector pUHA267 (▽, green yellow), and Δ*alr* complemented with MSMEG_5795 driven by the wild-type promoter (◆, blue) last two curves hidden by flat tracing for Δ*alr* growth.

Hours of incubation are plotted along the x-axis with OD_{600} shown on the y-axis. Error bars represent one standard deviation.

Figure 8: Purification and kinetic characterization of MSMEG_5795

Characterization of the gene product of MSMEG_5795. (A) SDS-PAGE analysis of the overall purification of the MSMEG_5795 protein. M: Molecular weight marker with sizes indicated in kDa, W: Whole cell lysate, S: Soluble protein, I: Sample pooled after immobilized metal affinity chromatography, G: Sample pooled after size exclusion chromatography. (B) Steady state kinetic parameters for the MSMEG_5795 protein using a coupled enzyme assay for D-amino acid transaminase were determined at substrate concentrations from 0.20-25.0 mM D-alanine. The average value of the duplicate measurements is shown for each substrate concentration with standard deviation shown as an error bar. Activity at substrate concentrations of 0.78 and 6.25 mM D-alanine were measured in triplicate. The velocity (in nM min^{-1}) was plotted against the substrate concentration (in mM), and used to determine the kinetic parameters for MSMEG_5795 with corresponding standard error. Each assay was performed at a final concentration of MSMEG_5795 of 77 nM. (C) Detection of glutamate production by mass spectrometry. Duplicates of the enzyme assays for D-amino acid transaminase were incubated for 20, 40 and 60 min and the amount of glutamate produced was measured as the ratio of peak intensities of singly protonated glutamate at m/z 148.060 versus the constant concentration of singly protonated aspartate at m/z 134.045 by direct infusion mass spectrometry. The concentration of glutamate was calculated based on a glutamate standard curve as described in Methods.

Figure 9: Growth phenotype of Δ*murI* strain with D-alanine

Growth curves of Δ*murI* strains complemented with D-alanine. Hours of incubation are plotted along the x-axis with OD_{600} shown on the y-axis. Error bars represent one standard deviation. Arrows indicate the point at which the cells were collected, washed and resuspended to remove any residual D-glutamate.

(A) The growth of wild-type (black curve), Δ*murI* (red curve), and Δ*murI* strain complemented with the *murI* gene (mustard curve) all without D-alanine supplementation.

(B) The growth of wild-type (black curve), Δ*murI* (red curve), and *murI* gene complemented strains (mustard curve) supplemented with 10 mM D-alanine.

Graphical abstract

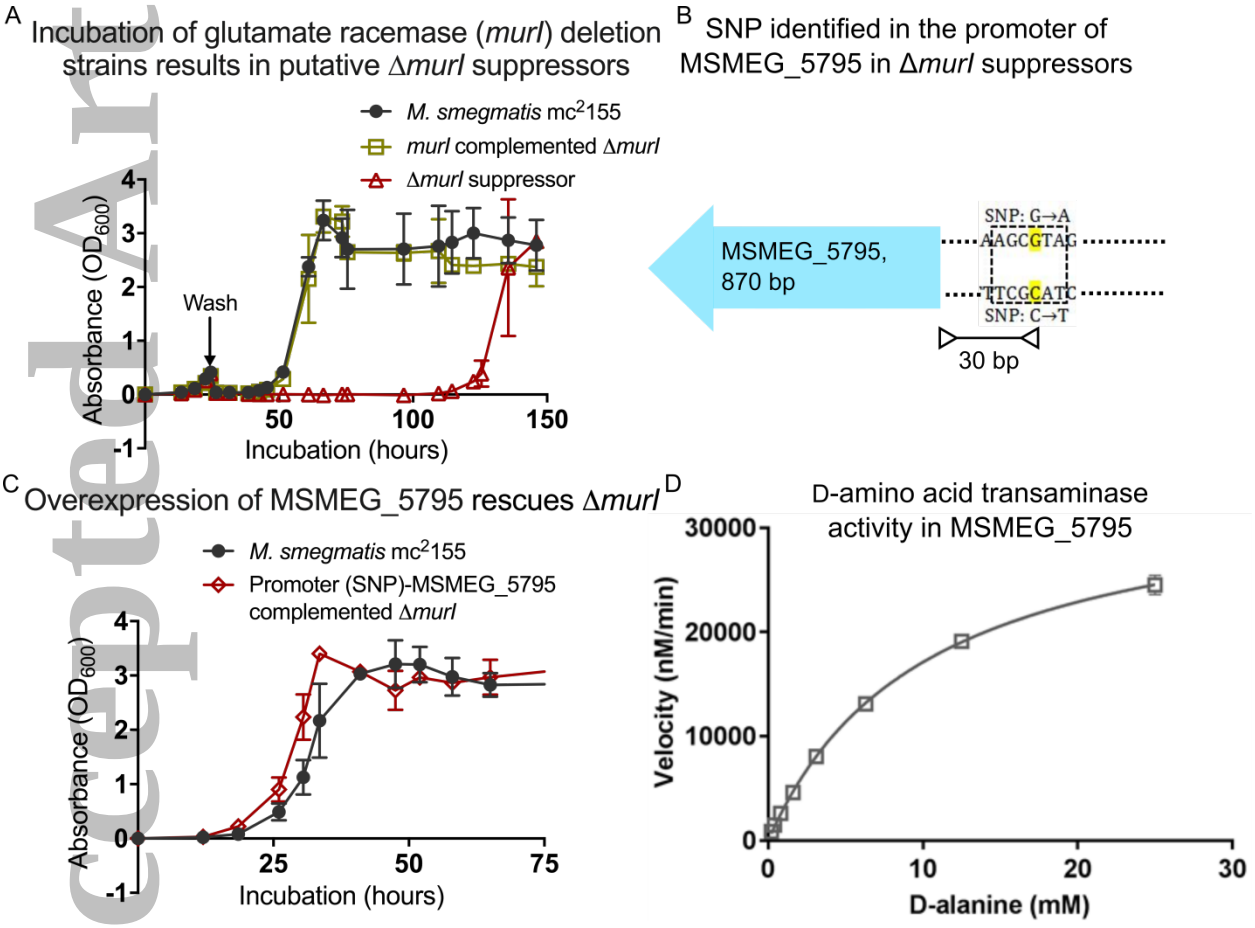

Summary Statement: Deletion of glutamate racemase (*murI*) in *M. smegmatis* is initially bacteriostatic, but following prolonged incubation, a revertant phenotype consistently develops, which is due to overexpression of MSMEG_5795. This gene is currently annotated as 4-amino-4-deoxychorismate lyase, but in this study, it is found to have D-amino acid transaminase activity. The MSMEG_5795 gene, with overexpression, is able to rescue deletion mutants of either glutamate racemase or alanine racemase and could play an important role in mycobacterial cell wall metabolism, and should be reannotated as a D-amino acid transaminase.

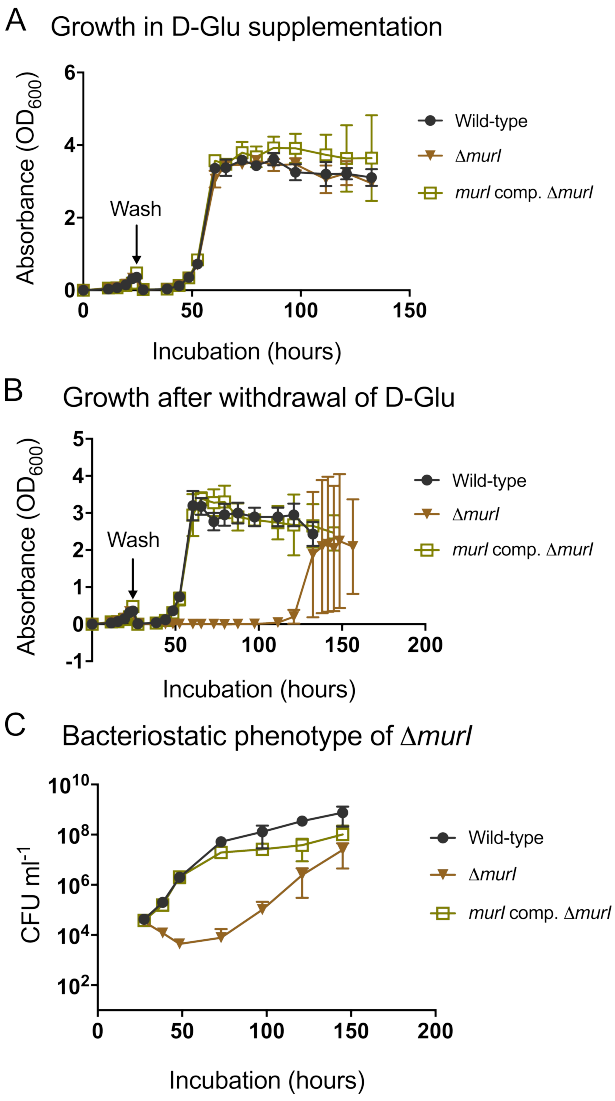

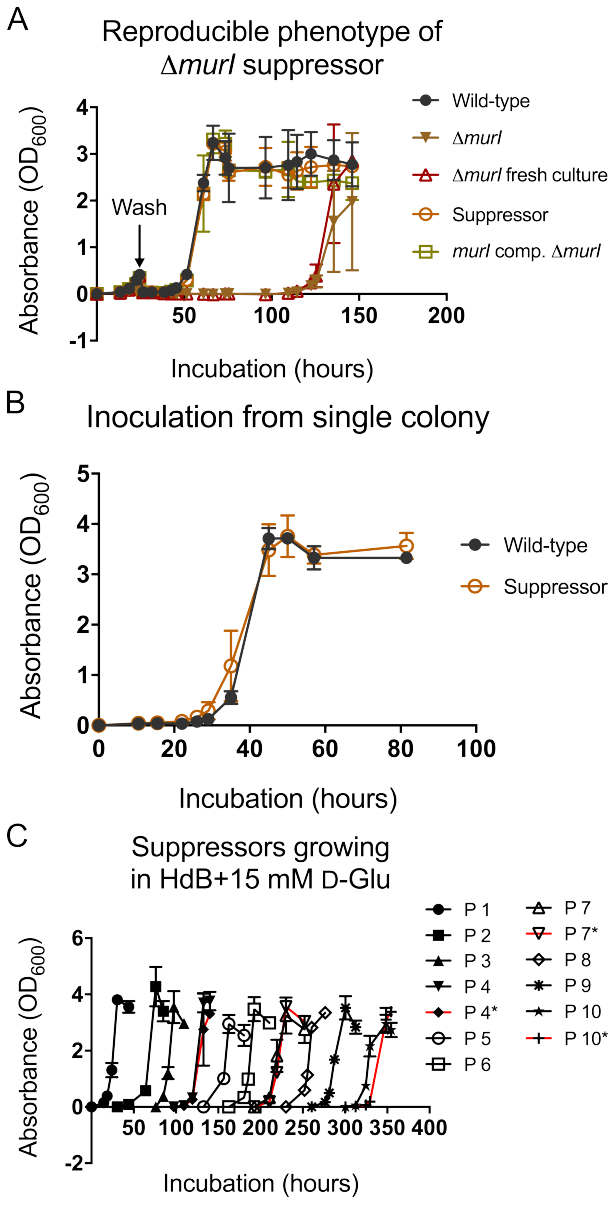

Figure 03

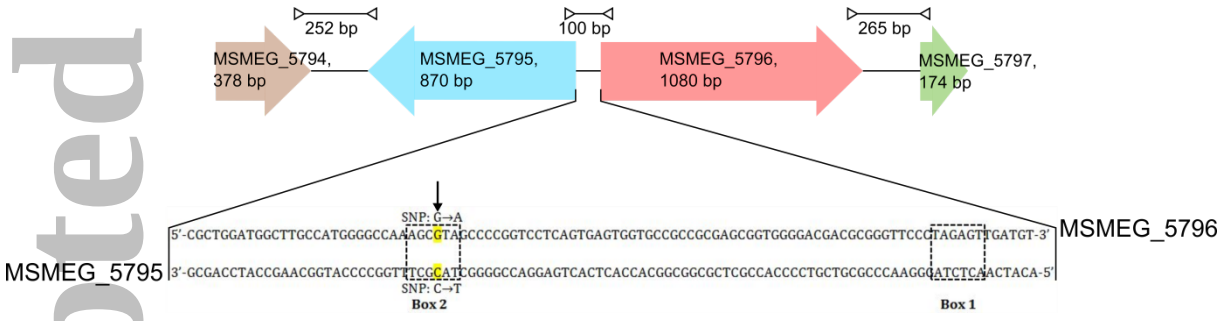

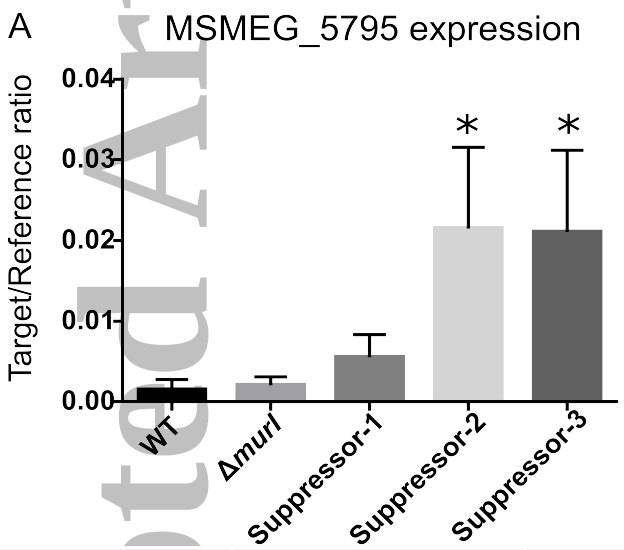

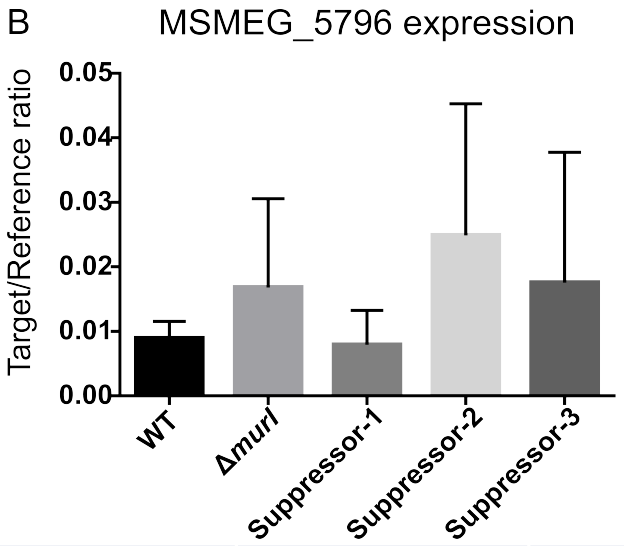

	MSMEG_5795	p-value
	Fold change	
WT	1	
Δ*murI*	1.39	0.58
Suppressor-1	3.73	0.09
Suppressor-2	14.55*	0.03
Suppressor-3	14.26*	0.03

	MSMEG_5796	p-value
	Fold change	
WT	1	
Δ*murI*	1.88	0.39
Suppressor-1	0.89	0.78
Suppressor-2	2.78	0.24
Suppressor-3	1.96	0.51

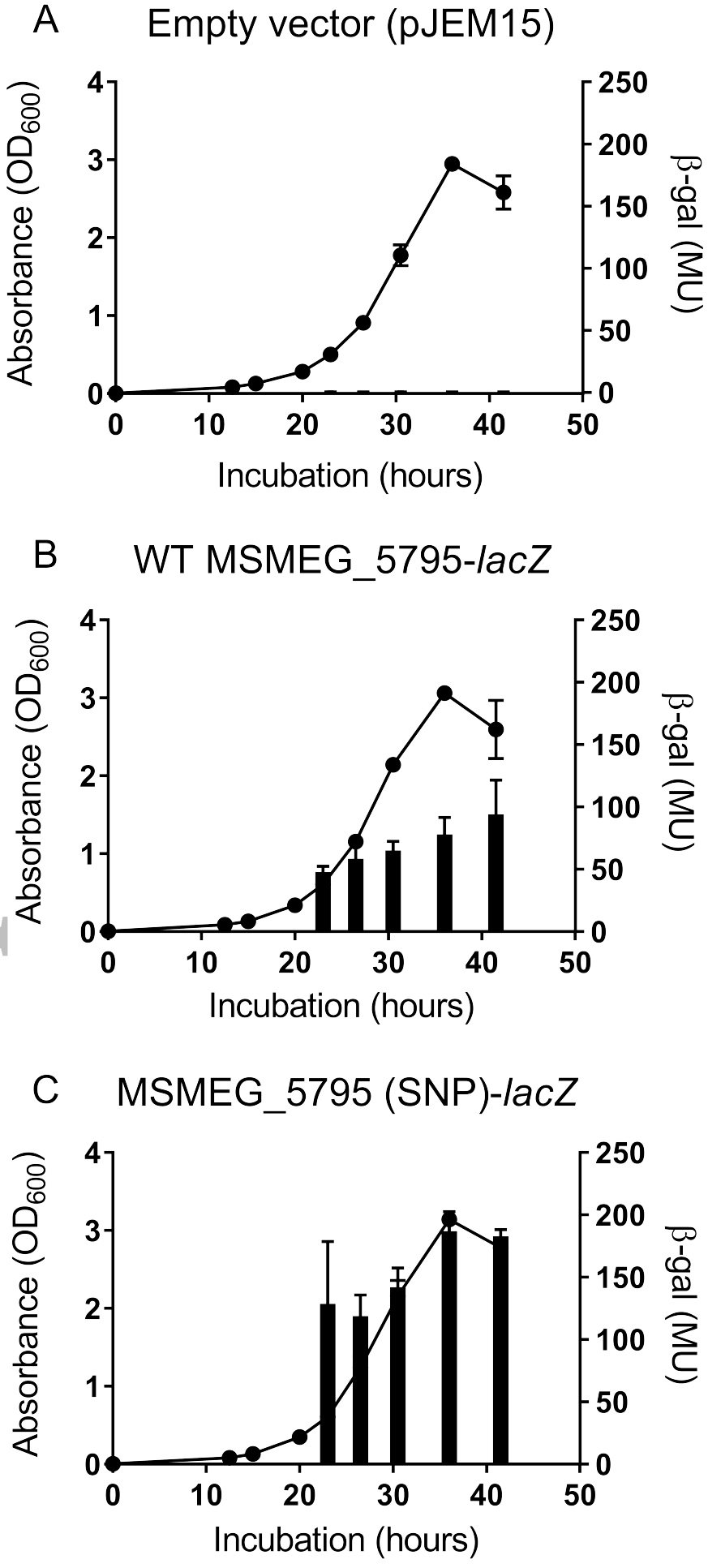

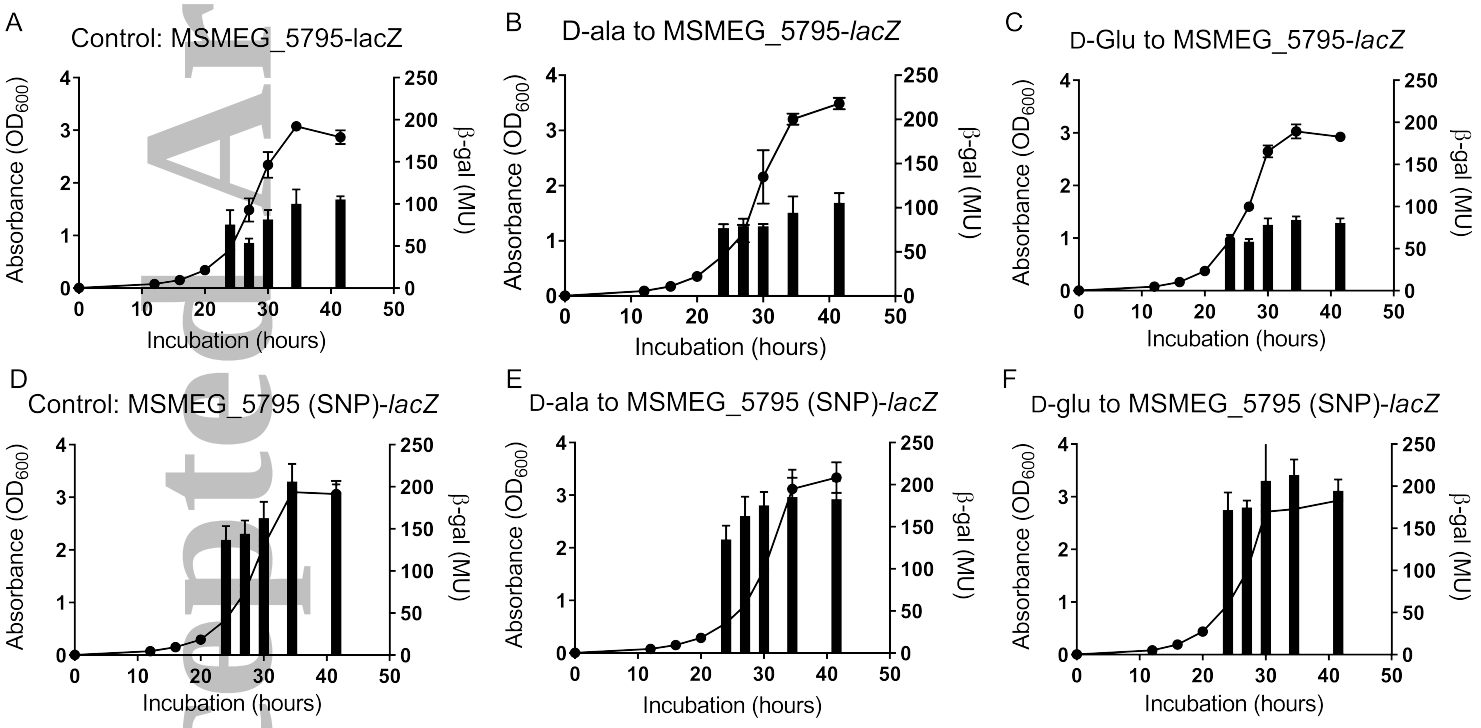

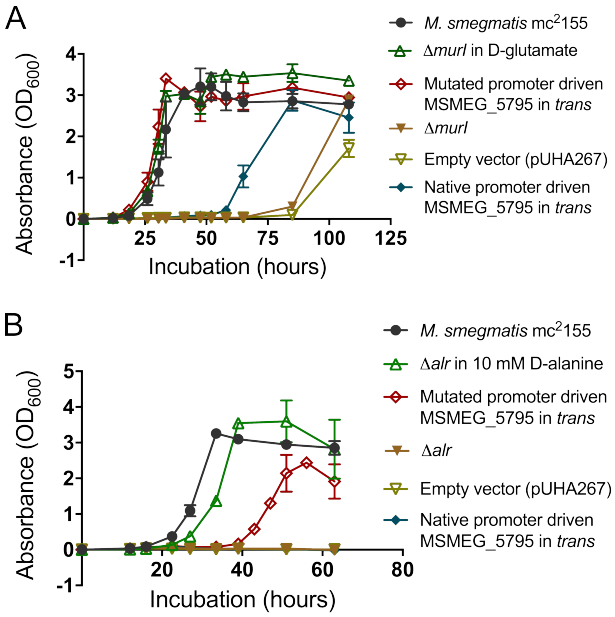

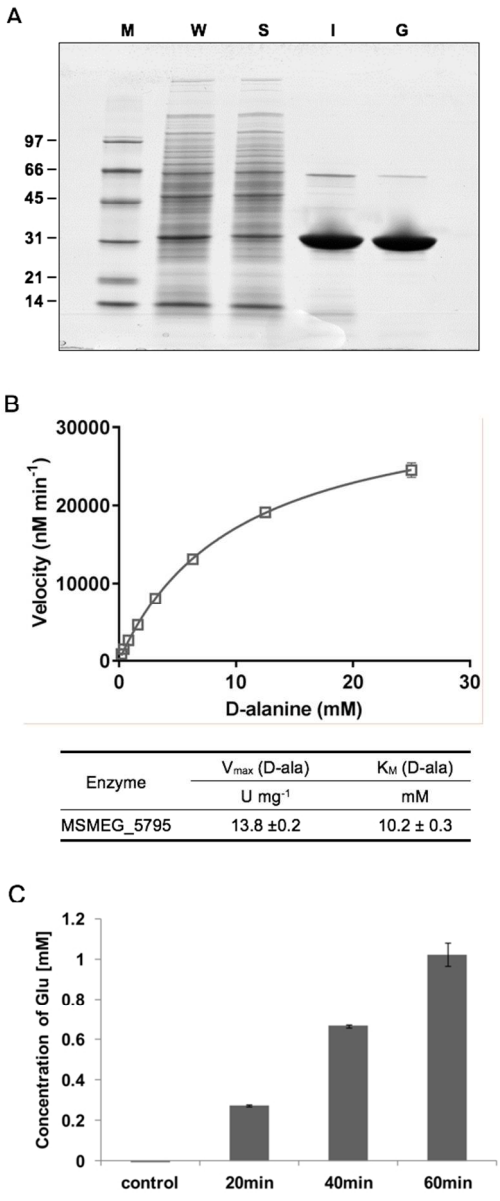

Enzyme	V_{max} (D-ala)	K_M (D-ala)
	U mg^{-1}	mM
MSMEG_5795	13.8 ±0.2	10.2 ± 0.3

Figure 8: Purification and kinetic characterization of MSMEG_5795

Characterization of the gene product of MSMEG_5795. (A) SDS-PAGE analysis of the overall purification of the MSMEG_5795 protein. M: Molecular weight marker with sizes indicated in kDa, W: Whole cell lysate, S: Soluble protein, I: Sample pooled after immobilized metal affinity chromatography, G: Sample pooled after size exclusion chromatography. (B) Steady state kinetic parameters for the MSMEG_5795 protein using a coupled enzyme assay for D-amino acid transaminase were determined at substrate concentrations from 0.20-25.0 mM D-alanine. The average value of the duplicate measurements is shown for each substrate concentration with standard deviation shown as an error bar. Activity at substrate concentrations of 0.78 and 6.25 mM D-alanine were measured in triplicate. The velocity (in nM min-1) was plotted against the substrate concentration (in mM), and used to determine the kinetic parameters for MSMEG_5795 with corresponding standard error. Each assay was performed at a final concentration of MSMEG_5795 of 77 nM. (C) Detection of glutamate production by mass spectrometry. Duplicates of the enzyme assays for D-amino acid transaminase were incubated for 20, 40 and 60 min and the amount of glutamate produced was

measured as the ratio of peak intensities of singly protonated glutamate at m/z 148.060 versus the constant concentration of singly protonated aspartate at m/z 134.045 by direct infusion mass spectrometry. The concentration of glutamate was calculated based on a glutamate standard curve as described in Methods.

209x484mm (72 x 72 DPI)